INVESTIGATING THE STRUCTURE OF THE 80-140KM REGION ON MARS. T.L. McDunn[1], S.W. Bougher[2], M.D. Smith[3], J.L. Bertaux[4], F. Montmessin[5], F. Forget[6], B.M. Steers[7], [1]U. of Michigan (2455 Hayward Avenue, Ann Arbor, MI 48109, tmcdunn@umich.edu), [2]U. of Michigan (2455 Hayward Avenue, Ann Arbor, MI 48109, bougher@umich.edu), [3]NASA GSFC (Greenbelt, MD), [4, 5]Service D'Aéronomie (France), [6]Laboratoire de Météorologie Dynamique [7]U. of Michigan (Ann Arbor, MI).

Motivation: Recently there has been a significant increase in the number of datasets available for the Martian middle atmosphere (~80-140 km). There has been some work using these new datasets, but there is still much that can be done to advance our understanding of Mars' middle atmosphere physical processes using these data.

This investigation characterizes the mean and wave structure of the middle atmosphere using density observations from the Mars Express SPectroscopy for the Investigation of the Characteristics of the Atmosphere of Mars (MEX/SPICAM) stellar occultations. Model-verification of the coupled MGCM-MTGCM at middle altitudes is also performed by comparing simulated densities with the observed densities. Finally, the SPICAM data is used to constrain this coupled multi-dimensional model, facilitating exploration of the underlying physical processes controlling the structure of the middle atmosphere.

MEX/SPICAM Dataset: MEX/SPICAM Stellar occultation density and temperature profiles (~70-140 km) have been obtained from F. Forget at the Laboratoire de Météorologie Dynamique (LMD). The SPICAM instrument is a UV-IR dual spectrometer. The instrument performs stellar occultations from which atmospheric densities are extracted [1], [2].

Model Description: The coupled NASA Ames MGCM and Michigan MTGCM framework is the principal numerical tool utilized to address the dynamical and thermal processes linking the Mars middle atmosphere with the lower and upper atmospheres and to interpret the MEX/SPICAM dataset. The MTGCM is a finite difference primitive equation model at the U. of Michigan that self-consistently solves for time-dependent neutral temperatures, neutral-ion densities, and three component neutral winds over the globe [3], [4], [5]. The MTGCM is currently driven by the NASA Ames MGCM code [6] at the 1.32 microbar level (near 60-80 km), permitting a detailed coupling across this boundary.

Dust History: Dust records from the ODYSSEY/THEMIS instrument indicate that dust loads for the aphelion season are relatively consistent from one Mars Year to the next (Fig. 1). Conversely, dust loads for the perihelion season display wide variability from one Mars Year to the next. The SPICAM dataset was taken during Mars Year 27, which, inspection of the THEMIS record indicates, was a year of low dust loading near the equator. Dust distributions measured by THEMIS [7] have not yet been tabulated and therefore dust loads from the MGS/TES instrument [8] are used to force the MGCM in the lower atmosphere (Fig. 2).

Model Results: The MGCM-MTGCM is currently run for 12 seasonal timeframes (L_s = 0, 30, 60, etc.). I have grouped the density observations into the same seasonal bins and identified the two areas (~20º latitude by 2 hours L_{st}) with the densest concentration of observations, for each seasonal bin.

For each of these regions I compare the observations within the area with the MGCM-MTGCM profile corresponding to the centroid of the region. The model captures the observed density structure in the middle atmosphere for several locations (Fig. 3). For selected locations, however, a height offset is required bring modeled densities into agreement with the observations.

To explore the seasonal structure and trends of densities in the middle atmosphere, I perform a model run using the appropriate L_s bin as well as the specific latitude and L_{st} corresponding to each set of SPICAM observations. I then compare these "best fit" model runs with their respective SPICAM observations over specified latitude ranges at 4 altitude levels, in a manner similar to the comparisons between SPICAM densities and LMD GCM outputs performed by *Forget, et al.* [9], [10]. The model performs well during the low-dust aphelion season, capturing the spread of density observations (Fig.4).

Similar comparisons are then carried out during the perihelion dust season employing modeled densities calculated for both low dust distributions and high dust distributions (TES Year 1 and TES Year 2, respectively). The model's accuracy and ability to capture the range of densities increases significantly when using enhanced dust loads (Fig. 5). From this it is determined that dust loads, which affect the thermal structure of the lower atmosphere, largely influence densities in the middle atmosphere. Hence, correct specification of dust distribution is critical to model performance and may remove the need to introduce height offsets to

bring modeled densities into agreement with observed densities.

Summary: Recent datasets now make it possible to study the middle atmosphere in more detail than has occurred previously. We investigate and characterize the density structure of the Mars middle atmosphere using the SPICAM dataset. Then, we compare the observed densities with model outputs to verify and constrain the coupled MGCM-MTGCM and uncover the physics forcing the motions of this portion of the atmosphere

Figures:

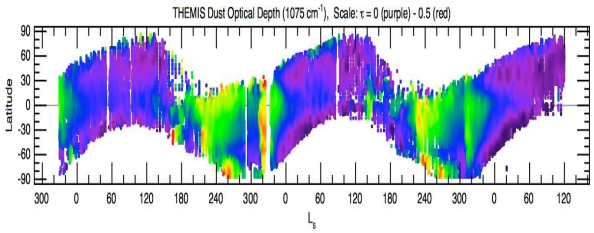

Figure 1. THEMIS dust record: Martian lower atmosphere dust opacities as a function of latitude for Ls = 330, Mars Year 25 through Ls = 120, Mars Year 28 [7].

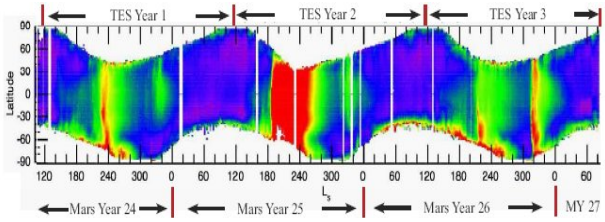

Figure 2. TES dust record: Martian lower atmosphere dust opacities as a function of latitude for Ls = 120, Mars Year 24 through Ls = 81, Mars Year 27 [11].

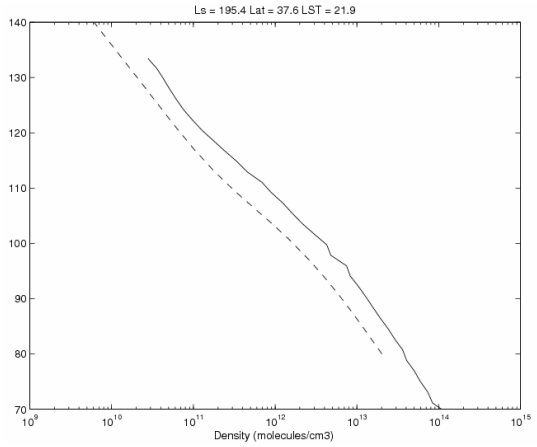

Figure 3. Observed-vs.-modeled density profiles: solid line represents observed data from MEX/SPICAM, dashed line represents MGCM-MTGCM simulations for the same L_s, Lat. and L_{st}. Here, while the model slightly underpredicts the densities, it captures the vertical structure of the observed density profile.

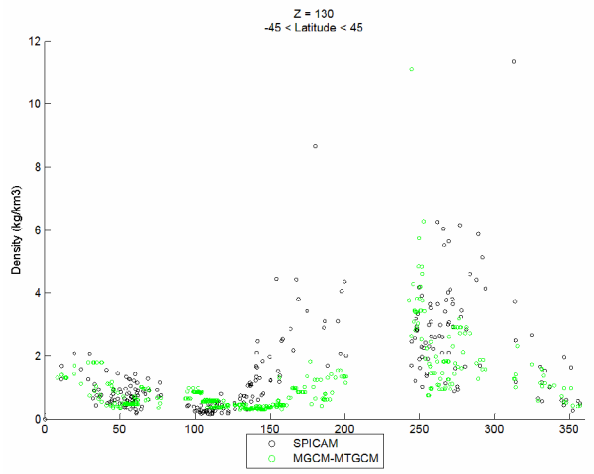

Figure 4. Seasonal structure and trends in density for the region between -45 degrees latitude and 45 degrees latitude at 130 km. Here, the model performs well during the low-dust season (L_s = 0 – 120).

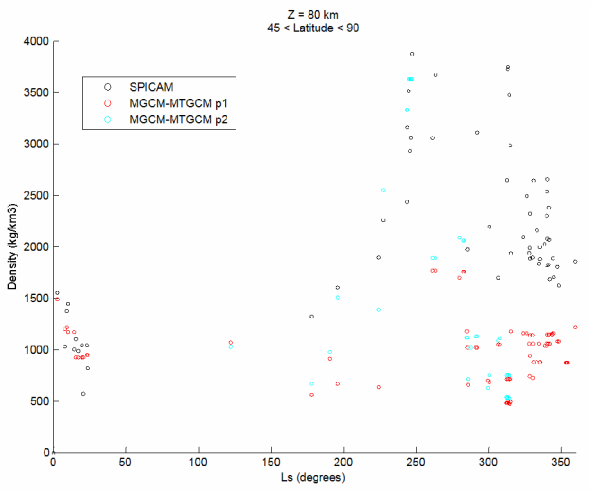

Figure 5. Seasonal structure and trends in density for the region between 45 degrees latitude and 90 degrees latitude at 80 km. Model-calculated densities are shown for both low dust conditions (TES Year 1, displayed in red) and high-dust conditions (TES Year 2, displayed in cyan). As can be seen, model performance improves when enhanced dust loads are employed.

References:

[1] Bertaux, J. L. (2006) *JGR, 111, E10S90.*
[2] Quemerais, E., et al. (2006) *JGR, 111, E9.*
[3] Bougher, S. W., et al. (1999) *JGR, 104, E7.*
[4] Bougher, S. W., et al. (2000) *JGR, 105, E7.*
[5] Bougher, S. W, et al. (2006) *GRL, 33, L02203.*
[6] Haberle, et al. (1999) *JGR, 104, E4.*
[7] Smith, M. D. (2007) *Private Communication*.
[8] Smith, M.D. (2004) *Icarus, 167.*
[9] Forget, et al. (2006) *IAA, Proceedings.*
[10] Forget, et al. (2007) *7th Mars, Abstract.*
[11] Bell, J.M., S.W. Bougher, and J.R. Murphy. (2007) *JGR (in review).*